

UCSF

UC San Francisco Previously Published Works

Title

Systemic inflammation regulates microglial responses to tissue damage in vivo

Permalink

<https://escholarship.org/uc/item/600007mm>

Journal

Glia, 62(8)

ISSN

0894-1491

Authors

Gyoneva, Stefka
Davalos, Dimitrios
Biswas, Dipankar
[et al.](#)

Publication Date

2014-08-01

DOI

10.1002/glia.22686

Peer reviewed



Published in final edited form as:

Glia. 2014 August ; 62(8): 1345–1360. doi:10.1002/glia.22686.

Systemic inflammation regulates microglial responses to tissue damage *in vivo*

Stefka Gyoneva^{1,2}, Dimitrios Davalos³, Dipankar Biswas⁴, Sharon A. Swanger¹, Ethel Garnier-Amblard^{1,5,6}, Francis Loth⁴, Katerina Akassoglou^{3,7}, and Stephen F. Traynelis¹

¹Department of Pharmacology, Emory University School of Medicine, Atlanta, GA 30322

³Gladstone Institute for Neurological Disorders, University of California at San Francisco, San Francisco, CA 94158

⁴Department of Mechanical Engineering, University of Akron, Akron, OH 44325

⁵Department of Chemistry, Emory University School of Medicine, Atlanta, GA 30322

⁷Department of Neurology, University of California at San Francisco, San Francisco, CA 94143

Abstract

Microglia, the resident immune cells of the central nervous system, exist in either a “resting” state associated with physiological tissue surveillance or an “activated” state in neuroinflammation. We recently showed that ATP is the primary chemoattractor to tissue damage *in vivo* and elicits opposite effects on the motility of activated microglia *in vitro* through activation of adenosine A_{2A} receptors. However, whether systemic inflammation affects microglial responses to tissue damage *in vivo* remains largely unknown. Using *in vivo* two-photon imaging of mice, we show that injection of lipopolysaccharide (LPS) at levels that can produce both clear neuroinflammation and some features of sepsis significantly reduced the rate of microglial response to laser-induced ablation injury *in vivo*. Under pro-inflammatory conditions, microglial processes initially retracted from the ablation site, but subsequently moved toward and engulfed the damaged area. Analyzing the process dynamics in 3D cultures of primary microglia indicated that only A_{2A}, but not A₁ or A₃ receptors, mediate process retraction in LPS-activated microglia. The A_{2A} receptor antagonists caffeine and preladenant reduced adenosine-mediated process retraction in activated microglia *in vitro*. Finally, administration of preladenant before induction of laser ablation *in vivo* accelerated the microglial response to injury following systemic inflammation. The regulation of rapid microglial responses to sites of injury by A_{2A} receptors could have implications for their ability to respond to the neuronal death occurring under conditions of neuroinflammation in neurodegenerative disorders.

Keywords

neuroinflammation; microglia; A_{2A} receptors; imaging; motility

Corresponding author: Dr. Stephen F. Traynelis, Emory University School of Medicine, Department of Pharmacology, Rollins Research Center Rm 5025, 1510 Clifton Rd. NE, Atlanta, GA 30322; Tel.: (404) 727-0357, Fax: (404) 727-0365; strayne@emory.edu.

²Current affiliation: Department of Neurosciences, Lerner Research Institute, Cleveland Clinic Foundation, Cleveland, OH 44195

⁶Current affiliation: RFS Pharma LLC., Tucker, GA 30084

Introduction

Neurodegenerative diseases such as Alzheimer's disease (AD), multiple sclerosis (MS), and Parkinson's disease (PD) are characterized by slow, progressive neuronal death. Despite the differences in neuronal populations affected in the diseases, one feature they share is the presence of ongoing neuroinflammatory processes (Akiyama et al. 2000; Prinz et al. 2011; Tansey and Goldberg 2010). Systemic inflammation can influence the progression of autoimmune diseases like MS and neurodegenerative diseases like AD and PD (Cunningham 2013; Murta and Ferrari 2013; Perry et al. 2007). In contrast, blocking inflammation with non-aspirin non-steroidal anti-inflammatory drugs (NSAIDs) is associated with reduced risk for developing AD and PD (Etminan et al. 2003; Gao et al. 2011), further supporting the involvement of the immune system in disease progression.

Microglia are the central nervous system's resident immune cells (Hanisch and Kettenmann 2007), but also perform important functions that help maintain normal activity in the healthy brain (Kettenmann et al. 2013; Tremblay et al. 2011). Time-lapse two-photon (2P) microscopy in living animals shows that microglia are highly motile, typically move their processes in a stochastic multi-directional pattern, and appear to monitor the brain parenchyma in the absence of a stimulus (Davalos et al. 2005; Haynes et al. 2006; Nimmerjahn et al. 2005); this type of motion is herein referred to as baseline motility or dynamics. Yet, when challenged by localized injury, microglial process movements are no longer stochastic, but extend directly toward the damaged region to contain the spread of cellular debris (Davalos et al. 2005).

Microglia show morphological and functional diversity in the brain, ranging from the ramified, "resting" phenotype associated with tissue surveillance in the healthy brain to amoeboid, cytokine-secreting and phagocytic phenotypes in disease states (Colton and Wilcock 2010). These "activated" microglia, visualized with PET imaging in patients, are present at much higher levels at sites of neurodegeneration in AD, PD and MS patients compared to healthy age-matched controls (Edison et al. 2008; Gerhard et al. 2006; Venneri et al. 2013). Interestingly, the purinergic P2Y₁₂ receptor that microglia use to sense ATP released at sites of tissue damage is down-regulated following microglial activation (Haynes et al. 2006; Orr et al. 2009). This is accompanied by up-regulation of the adenosine A_{2A} receptor (Orr et al. 2009), which can be activated indirectly by ATP after its rapid breakdown to adenosine. In contrast to the ability of ATP to induce process extension and chemoattraction in resting microglia (Davalos et al. 2005; Honda et al. 2001), ATP induces process retraction in activated microglia *in vitro* in an A_{2A} receptor-dependent manner (Orr et al. 2009).

The lack of P2Y₁₂ receptors and the differential effect of ATP in activated microglia *in vitro* make it uncertain how activated microglia will respond acutely to an ATP gradient in the moments after neuronal death as it occurs in neurodegenerative diseases. Yet, there are virtually no data assessing the regulation of microglial motility in real time by systemic inflammation or activation of A_{2A} receptors *in vivo*. Thus, we performed *in vivo* 2P imaging of microglia in lipopolysaccharide (LPS)-treated mice, a model of peripherally-induced neuroinflammation as well as septic insult, to determine microglial response to tissue

damage and cell death. We also examined the involvement of other adenosine receptors (A_1 , A_3) in modulating microglial process dynamics *in vitro* to elucidate whether they may mediate the effects of physiologic ATP-derived adenosine *in vivo*. Our results show for the first time *in vivo* that the presence of peripherally induced neuroinflammation changes both microglial baseline activity and approach to tissue damage. Ultimately, this could affect the cells' surveillance and clearance functions in the unperturbed and damaged brain, respectively.

Materials and Methods

Reagents

Ligands for purinergic receptors were purchased from Sigma (ATP, ADP β S, adenosine, CGS-21680, caffeine) or Tocris (2'-MeCCPA, 2-Cl-IB-MECA). Stock solutions were prepared in de-ionized water (ATP, adenosine, ADP β S, caffeine) or DMSO (CGS-21680, 2'-Me-CCPA, 2-Cl-IB-MECA, preladenant; 0.1% v/v final DMSO concentration). Preladenant was synthesized and prepared in 50% polyethylene glycol-400 for mouse injections as described (Hodgson et al. 2009). *In vitro* activation of microglia was achieved with LPS from *E. coli* strain O26:B6 (Sigma, L2654), while LPS from *E. coli* K-235 (Sigma, L2143) was used for mouse injections.

Animals and primary microglia culture

All procedures involving the use of animals were approved by the Institutional Animal Care and Use Committees at Emory University and the University of California, San Francisco. Microglia (>95% pure, assessed by IB₄ staining) were obtained from astrocyte co-cultures after triturating the cortices of P0–P4 pups as previously described (Orr et al. 2009). Microglia for confocal imaging experiments were prepared from *actin-GFP* mice (provided by M. Okabe, Osaka University, Japan) that express enhanced green fluorescent protein (GFP) in all cells from the actin promoter. $CX_3CR1^{GFP/GFP}$ mice that exhibit microglia-specific GFP expression (Jung et al. 2000) were purchased from Jackson Laboratories and bred in-house to generate $CX_3CR1^{GFP/+}$ mice used for *in vivo* imaging. Both males and females were used for experiments.

RT-PCR

Total cellular RNA was isolated from primary microglia using the PureLink RNA Mini Kit (Invitrogen). The RNA was treated with 2 U/reaction DNase I (Invitrogen) to remove contaminating DNA. Semi-quantitative reverse transcriptase-PCR was carried out with 50 ng RNA as template using the SuperScript III One-Step RT-PCT System with Platinum *Taq* DNA Polymerase (Invitrogen). The protocol included incubation at 60°C for 30 min for cDNA synthesis before amplification. Primer sequences and amplification conditions for IL-1 β , TNF- α and β -actin are published elsewhere (Tha et al., 2000; Bianco et al., 2005).

FluoroJade Staining

To determine if peripheral LPS treatment induces cell death in the brain, we performed FluoroJade staining (Jiang et al. 2013). $CX_3CR1^{GFP/+}$ mice were injected with 2 mg/kg LPS or PBS and euthanized two days later. The brains were drop-fixed in 4% paraformaldehyde,

cryoprotected in 30% sucrose and sectioned on a cryostat at 20 μm thickness. For staining, the sections were mounted on slides and air dried. Because the emission of GFP overlaps with the emission of FluoroJade, GFP fluorescence was quenched by incubating the slices in 2N HCl for 30 min (37°C). The acid was neutralized by washing for 2 \times 5 min with 0.1M borate buffer (pH 8.5) and then 3 \times 5 min with distilled H₂O (dH₂O). Then, the sections were incubated in 0.06% potassium permanganate for 10 min, washed with dH₂O, and transferred to 0.001% FluoroJade in 0.1% acetic acid for 10 min. After a final wash in dH₂O, the sections were air-dried and coverslipped. As positive control, we stained sections from pilocarpine-treated animals (180 mg/kg i.p.), which is known to induce cortical cell death [Jiang et al. (2013); sections were provided by Dr. Nicholas Varvel]. After staining, images were obtained with an Olympus BX51 confocal microscope.

Two-photon imaging

Imaging of the cortex of anesthetized 2–5 month old *CX₃CR1^{GFP/+}* mice was performed as previously described (Davalos et al. 2005). To study microglial motility under pro-inflammatory conditions, mice were injected with 2 mg/kg LPS i.p. This LPS dose is similar to those typically used to model sepsis [5–10 mg/kg; Semmler et al. (2007); Semmler et al. (2008); Semmler et al. (2005); Weberpals et al. (2009)], and resulted in 15.4% mortality in *CX₃CR1^{GFP/+}* mice but no detectable cell death in the cortex (see Figure-1). Two days later, the mice were anesthetized with 200 mg/kg ketamine and 30 mg/kg xylazine in 0.9% NaCl and prepared for imaging by thinning the skull to 50 μm thickness to create an imaging window (~1 mm diameter) over the somatosensory cortex. Two multiphoton microscopes, both employing Spectra Physics MaiTai DeepSee Ti-sapphire lasers, were used: a Prairie Technologies Ultima IV and an Olympus Fluoview 1000MPE microscopes. 3D image stacks were obtained using an Olympus 40 \times 0.8NA water immersion lens and 1.5X optical zoom. Each imaging session consisted of a baseline recording, laser ablation and recording of microglial responses to the ablation. Stacks spanning 30–40 μm vertical distance of the cortex (~1 μm step between optical planes) were acquired every 30 s for 10 min to record baseline process motility. Laser ablations with diameter of ~20 μm were induced by focusing a high-energy laser beam (800 nm wavelength for 0.5–2 s, depending on bone thickness). Subsequent imaging (60 min total duration, 3 min intervals between stack acquisitions) allowed for the detection of microglial responses to injury. Time-lapse imaging of microglial responses to laser injury began ~2–3 min after its induction to allow the restoration of imaging parameters on the multiphoton laser.

To examine the effects of preladenant on process motility *in vivo*, mice were first injected with 2 mg/kg LPS i.p. and imaged two days later as above. After conclusion of the first imaging session, mice were injected with 3 mg/kg preladenant. A second imaging session, consisting of both a baseline recording and second laser ablation, was performed ~1 hr following the preladenant injection to allow the compound to distribute throughout the body (Neustadt et al. 2007). In this way, we had recordings before and after preladenant treatment in the same animal.

Although skull thinning was performed in the same way, the intensity of the detected fluorescence varied between animals depending on depth of imaging field, thickness of the

skull, and chosen exposure time. As a result, poor signal-to-noise ratio in some animals prevented clear visualization of microglial processes. Image stacks from animals with average fluorescence intensity <25 arbitrary units – empirically determined as our minimum threshold, measured with ImageJ on the first frame of each stack – were eliminated from all analyses. Three control, one LPS, and no preladenant-treated animals were excluded from analysis.

Image analysis

Time-lapse 2P sequences capturing baseline motion or response to laser ablation were analyzed in different ways. First, Imaris v7.6 software (Bitplane AG, Switzerland) was used to quantify the baseline process motility patterns of microglia in the absence of tissue damage. Following 3D recreations of the imaged volumes, the software detected objects with diameter larger than 2 μm and tracked them over time with an Autoregressive Motion GapClose algorithm (max distance of 5 μm) to determine the average length and speed of movement (regardless of direction) over the full duration of the recording. The size of microglial cell bodies and number of primary branches were quantified with ImageJ software (National Institutes of Health) from 2D projections of the imaged volume. The cell bodies that were fully within the imaging field were manually outlined, and the area of the resulting region of interest was measured. Similarly, the primary branches of cell bodies that were fully within the imaging field were manually counted.

Second, time-lapse recordings of microglial responses to laser ablations were quantified with MGPtracker, a custom-written code implemented in Matlab (MathworksTM, Natick, MA) that allowed us to measure the radial movement of microglial processes in response to tissue damage. Initially, ImageJ software was used to determine the threshold fluorescence that distinguishes fluorescent microglia from background with the MaxEntropy thresholding function in maximum-intensity 2D projections. There are no significant differences in the threshold values between the compared groups, indicating that the fluorescence intensities of the different recordings were similar (data not shown). The 2D time sequences were then analyzed with MGPtracker, which converts the recordings to binary (black-and-white) images by applying the previously determined thresholds. It then detects the microglial processes closest to the ablation (circle of autofluorescence close to the middle of the image) at 10° angles; the positions of these processes form the vertices of a polygon that represents a front of microglial processes that will respond to the damage, and averaging all vertices for a given time point represents the average distance from the ablation of the microglial processes at that time point. Repeating the calculations for each time point gives the approach waveform for each animal over time. Two different parameters were calculated: the average distance of microglial processes from the ablation, and the size of the area surrounding the ablation bound by the polygon. Finally, the time when microglial processes reach the ablation site was calculated as the average of the times when individual vertices on the polygon reached the ablation; if a vertex never reached the ablation, its time was considered to be 60 min.

Confocal imaging of primary microglia in vitro

Microglial process dynamics were studied in Matrigel (BD Biosciences) with confocal imaging as described (Orr et al., 2009; Gyoneva and Traynelis, 2013). When necessary, microglia were activated with 100 ng/mL LPS for 24 hr. The imaging protocol included a baseline reading to establish resting motility, application of specified treatments, and washout. Z-plane stacks were acquired every 30 s, and the resulting time sequences were analyzed with Imaris software. Following background subtraction (10 μ m filter), 3D representations of the cells were generated from the z-stacks and smoothed with 0.250 μ m Gaussian algorithm. To measure changes in cell ramification, the surface area-to-volume ratio was calculated at each time point, which has been shown to correspond to changes in process velocity (Orr et al. 2009) and process length (Gyoneva and Traynelis 2013).

Statistical analysis

All time-lapse recordings for imaging experiments were given non-descriptive names consisting of date and number; the researcher was blind to the treatment of each recording during image analysis. Recordings were performed in random order of control and experimental conditions. Whenever appropriate, the measures under study were quantified and plotted as averages \pm standard error of the mean (SEM). Statistical tests were performed in SigmaPlot v11.0 and GraphPad Prism v5. For each experiment, the sample sizes and appropriate tests [ANOVA, repeated measures- (RM-) ANOVA, *t*-test, etc.] are indicated in the figure legends. The G-test of independence, a variant of the chi-square test that compares the frequency of one nominal variable in a population to a second variable to determine if they are independent (McDonald 2009), was used to analyze the distributions of events after certain treatments (see Figure-4E, 8E). Results were considered to be significantly different if $p < 0.05$.

Results

Characterization of activated microglia in vivo

The bacterial cell wall component LPS can induce central nervous system inflammation after a single peripheral injection (Qin et al. 2007), and has been used to model a range of conditions from neuroinflammation at low doses (0.5–1 mg/kg) to sepsis (5–10 mg/kg). In the current study, we treated *CX₃CR1^{GFP/+}* mice with 2 mg/kg i.p. LPS. Two days post-injection there was increased mRNA expression of the pro-inflammatory cytokines IL-1 β and TNF- α (Figure-1A) in cortical tissue. Evaluation of FluoroJade staining confirmed that this LPS-induced neuroinflammation did not lead to detectable cell death in the brain at this time point (Figure-1B). As a positive control for staining, cell death was detectable in the cortex of pilocarpine-treated mice (Figure-1B; Suppl. Figure-1).

Thus, we selected 48 hours post-injection to perform *in vivo* 2P microscopy with the thinned skull preparation that is commonly used to study microglial behavior in the healthy brain (Davalos et al. 2005; Haynes et al. 2006; Nimmerjahn et al. 2005). We first examined the morphological characteristics of microglia in the brain. Analysis of the *in vivo* imaging data showed that microglia in LPS-injected mice had altered morphology (Figure-1C) characterized by significantly larger cell bodies (Figure-1D; Student's *t*-test, $p = 0.003$) and

higher number of primary processes (Figure-1E; Student's *t*-test, $p < 0.001$). The coverage of the brain parenchyma by microglial processes also appeared altered: whereas microglial processes in control animals are uniformly spaced throughout the whole parenchyma, there were large gaps with seemingly process-free spaces in LPS-treated animals (Figure-1C).

After confirming the presence of neuroinflammation following LPS treatment, we examined the motility patterns of activated microglia both in the presence and absence of laser-induced tissue damage. Initially, we imaged microglia in the cortex of LPS-injected mice before induction of a laser ablation. Time-lapse recordings indicated that 48 hr after LPS injection activated microglia continued to sample the brain parenchyma by process extension and retraction (Suppl. Video 1). Quantification of the process motility patterns *in vivo* showed that microglia in control animals extended and retracted their processes at an average speed of $\sim 1 \mu\text{m}/\text{min}$, which is comparable to speeds seen in the healthy brain (Davalos et al. 2005). However, microglia in LPS-treated animals moved their processes at significantly higher mean instantaneous speeds than control microglia (Figure-2B; Student's *t*-test, $p = 0.0052$), which led to longer distances traveled over the 10-min period (Figure-2C; Student's *t*-test, $p = 0.0178$). These data indicate that the presence of inflammation itself alters microglial dynamics even in the otherwise uninjured brain, possibly affecting microglial monitoring of the brain parenchyma.

Response of activated microglia to tissue damage in vivo

In the healthy brain microglia respond to focal damage by extending their processes and surrounding sites of injury within minutes (Davalos et al. 2005; Haynes et al. 2006). Their ability to rapidly respond to localized brain damage is considered essential for maintaining normal brain function in the presence of daily physiological disturbances such as rupture of small blood vessels or death of individual cells (Hanisch and Kettenmann 2007). Considering the divergent effects of ATP on resting *vs.* activated microglia *in vitro* (Orr et al. 2009), we tested the ability of activated microglia in LPS-injected mice to respond to laser-induced tissue damage. In both control and LPS-treated animals microglial cells in the tissue around the laser ablation extended their processes toward the ablation site in the characteristic radial manner seen before (Davalos et al. 2005) (Figure-3A,B; Suppl. Video 2). To assess the radial motion quantitatively, we developed a custom algorithm in Matlab (referred to as MGPtracker) that automatically tracks the distance of the closest microglial processes as they converge from every direction around the ablation site. The algorithm then draws a polygon around the laser ablation, the vertices of which are the microglial processes closest to the ablation (Figure-4A,B; Suppl. Video 3; see Materials and Methods). To validate the ability of MGPtracker to capture radial motion, we compared the results obtained with MGPtracker to those obtained by manually measuring the distances of eight microglial processes arranged at 45° increments around the ablation site (data not shown). Despite the different number of vertices (8 *vs.* 36), the two curves had similar waveforms and showed similar trends, confirming that MGPtracker faithfully captured microglial responses toward the site of injury. Moreover, using MGPtracker we calculated additional parameters of the response, such as the area bound by the polygon and the time to reach the ablation.

Analysis of the average distance between microglial processes and the ablation showed that microglia in LPS-treated animals approached the ablation at a slower rate than microglia in control animals (Figure-4C; ANOVA, $F_{(1,360)}=44.74$, $p<0.0001$). Similarly, the area bound by the polygon, namely the area around the ablation that remains clear of microglial processes, was also significantly larger for LPS-treated animals compared to control throughout the time course of the response (Figure-4D; ANOVA, $F_{(1,360)}=103.6$, $p<0.0001$), also implying a slower response to the injury. It should be noted that microglia in LPS-treated animals exhibit an initial retraction from the ablation, which is seen in the increase in distance from the ablation (Figure-4C) and the cleared area (Figure-4D). This does not represent the chance detection by the algorithm of spaces devoid of processes in LPS-injected animals, as the distribution of distances was uniformly further from the injury in LPS-treated animals (data not shown). Moreover, the processes continued to retract for several time points after the injury, confirming that the increase in distance is not a function of the geometry surrounding the ablation in LPS-treated animals. Nine out of eleven LPS-injected mice displayed this type of biphasic response, but only one of nine control animals exhibited initial retraction (Figure-4E; G-test of independence, $p<0.001$). However, microglia in control and LPS-injected animals reached the ablation at similar times (Figure-4F; Student's *t*-test, $p=0.2531$), suggesting that inflammation *per se* does not prevent microglia from responding to laser-induced tissue damage.

Microglial process dynamics in vitro

The data presented above provide the first *in vivo* demonstration of process retraction from the site of injury, a phenomenon that to our knowledge has not been reported in the literature. We have previously shown that the activation of adenosine A_{2A} receptors can cause a similar phenomenon in primary microglia (Orr et al. 2009). However, this earlier study did not utilize the native agonist adenosine, which is liberated *in vivo* following breakdown of ATP (Davalos et al. 2005; Zimmermann 1994). Because adenosine can activate several subtypes of receptors, we used a series of subtype-selective pharmacological tools to extend our studies to the potential regulation of microglial process motility by adenosine A₁ or A₃ receptors.

Plating primary cortical microglia inside the gelatinous substrate Matrigel allows the cells to assume a three-dimensional, process-bearing morphology; changes in cell morphology can be studied with time-lapse confocal microscopy followed by 3D reconstructions of individual cells (Figure-5; Suppl. Video 4). Changes in cell ramification, measured as the ratio of surface area to volume at each time point, correspond to changes in microglial process motility (Orr et al. 2009). An increase in the length of the processes influences surface area more than volume and thus increases the ratio of surface area-to-volume; the opposite occurs for process retraction (Figure-5). Indeed, application of 20 μ M ATP caused process extension in control microglia, but process retraction in LPS-activated (100 ng/mL, 24 hr) microglia (Figure-6A,D). To further distinguish the relative contributions of different signaling pathways, we used selective agonists and antagonists for the various purinergic receptors. First, we selectively activated P2Y₁₂ receptors with 10 μ M ADP β S, a potent and non-hydrolysable agonist that cannot be broken down to adenosine (von Kugelgen and Wetter 2000). ADP β S induced process extension in resting microglia, but it had no effect on

the processes of LPS-activated microglia (Figure-6B,D). In contrast to the dual effects of ATP, 10 μ M adenosine, the physiological agonist for A_{2A} receptors, caused process retraction only in activated microglia (Figure-6C,D). These data are consistent with A_{2A} receptor activation by ATP breakdown products as suggested before (Orr et al. 2009).

Adenosine is the endogenous ligand for A_1 , A_{2A} and A_3 receptors, which are expressed on microglia (Fredholm et al. 2001; Hasko et al. 2005). Because A_1 and A_3 receptors can potentiate ATP-induced migration of resting microglia (Färber et al. 2008; Ohsawa et al. 2012), we employed receptor-selective agonists and antagonists to determine the contribution of each adenosine receptor subtype. The effects of adenosine on activated microglia appear to be mediated through A_{2A} receptors, as selective activation of adenosine A_1 or A_3 receptors with 1 μ M 2'-MeCCPA and 0.5 μ M 2-Cl-IB-MECA, respectively (Franchetti et al. 1998; Gallo-Rodriguez et al. 1994), did not change the process dynamics of LPS-activated microglia. In contrast, 3 μ M of the selective A_{2A} agonist CGS-21680 (Hutchinson et al. 1989) induced a significant degree of process retraction (Figure-6E,F). The lack of effect of 2'-MeCCPA and 2-Cl-IB-MECA was not due to their inability to activate their respective G_i -coupled receptors at the concentrations used, as control experiments show that they were able to inhibit forskolin-induced cAMP accumulation in a heterologous expression system (data not shown).

Finally, we examined the ability of A_{2A} antagonists to affect microglial process dynamics *in vitro*. Both the non-selective adenosine receptor antagonist caffeine [100 μ M; Fredholm et al. (2001)] and the selective A_{2A} receptor antagonist preladenant [1 μ M; Neustadt et al. (2007)] prevented the adenosine-induced process retraction in activated microglia (Figure-6G,H). Furthermore, there was no significant difference in the magnitude of the effects of preladenant and caffeine (Figure-6H; ANOVA and Tukey's *post hoc* test, $p=0.988$). These data, together with the lack of effect of A_1 and A_3 agonists on process motility, suggest that the effects of the non-selective antagonist caffeine are likely mediated through A_{2A} adenosine receptors. Overall, our *in vitro* data indicate that the A_{2A} receptor is the sole adenosine receptor inducing process retraction selectively in activated microglia, an effect that could be prevented by selective antagonism of A_{2A} receptors.

Effects of A_{2A} receptor antagonists on microglial motility in vivo

Because A_{2A} receptor antagonists can reverse ATP- (Orr et al. 2009) and adenosine-stimulated microglial process retraction *in vitro* (Figure-6G,H), we tested if preladenant, a highly selective and brain permeable A_{2A} antagonist (Neustadt et al. 2007), would ameliorate the delayed response to laser ablation in LPS-injected animals *in vivo*. Even though all animals receive the same LPS dose (2 mg/kg), individual animals might vary in intensity of inflammation and microglial activation. To reduce the effects of inter-animal variability, we performed two imaging sessions in the same LPS-injected animals, and evaluated both baseline motility and responses to laser injury before and after preladenant treatment (3 mg/kg, i.p.). It previously has been shown that there is no interference between closely spaced ablations (~50 μ m apart) even if they are separated in time by as little as 20 min (Davalos et al. 2005). Nevertheless, after the first imaging session was concluded and preladenant was administered, we conducted the second imaging session at a cortical area at

least 100 μm away from the first ablation site and performed the second ablation ~2 hr after the first one.

We first examined whether blocking A_{2A} receptors affected the baseline motility of microglia in the unperturbed brain. Preladenant application did not significantly change the baseline microglial process dynamics in terms of speed of movement (1.01 ± 0.026 and 1.01 ± 0.052 $\mu\text{m}/\text{min}$ before and after preladenant, respectively; Student's paired t -test, $p=0.9857$), and length of total distance traveled (3.89 ± 0.32 and 3.79 ± 0.29 μm before and after preladenant; Student's paired t -test, $p=0.8376$), indicating that A_{2A} receptors are not involved in the baseline motility of microglia under pro-inflammatory conditions.

We next compared the ability of activated microglia in LPS-treated mice to respond to tissue damage before and after A_{2A} receptor inhibition. Examination of the responses of individual animals was indicative of a differential microglial approach toward the ablation site following preladenant treatment (Figure-7A,B). Indeed, preladenant treatment had a significant effect on both the distance from the ablation site (Figure-8A; RM-ANOVA, $F_{(1,120)}=24.14$, $p<0.0001$), and the size of the process-cleared area surrounding the ablation (RM-ANOVA, $F_{(1,120)}=4.200$, $p=0.0426$; data not shown) when compared to the same animal before treatment. To determine if the presence of a pre-existing ablation alone might improve the response to a second ablation, we examined mice injected with PBS rather than preladenant between the two imaging sessions (Suppl. Figure 2). There was no significant effect of treatment in the distance from the ablation (Figure-8B; RM-ANOVA, $F_{(1,30)}=0.3032$, $p=0.5839$) or the area of the cleared region (RM-ANOVA, $F_{(1,60)}=0.2157$, $p=0.6440$; data not shown) between the two consecutive ablations. Moreover, preladenant treatment reduced the time required for microglial processes to reach the ablation in six out of seven animals (Figure-8C). Yet, if the mice received PBS treatment instead of preladenant before the second ablation, only one of four animals displayed a faster approach to the second ablation (Figure-8D). This represents a significant difference in terms of the qualitative response to injury in preladenant-injected animals compared to vehicle (Figure-8C-E; G-test of independence; $p=0.041$). Overall, the difference in the distance in the same animal before and after preladenant treatment (Figure-8A) and the different response of preladenant- and PBS-treated animals (Figure-8E) suggest that A_{2A} receptors are involved in microglial responses to tissue damage under pro-inflammatory conditions.

Discussion

Systemic inflammation, such as from pathogen infections, can affect the progression of AD, MS, and PD (Perry et al. 2007). In the present study, we induced systemic inflammation in order to study the motility of microglia in a model of neuroinflammation that had a peripheral origin. We performed the first comprehensive characterization of the baseline motility of activated microglia and their ability to detect and respond to tissue damage following peripheral immune system activation *in vivo*. Our data allowed us to draw three main conclusions: (1) systemic inflammation affects the baseline morphology and dynamics of microglia in the brain *in vivo*, (2) microglia in LPS-treated mice respond differently to tissue damage compared to microglia in healthy animals, (3) the A_{2A} receptor antagonist preladenant accelerates the approach of activated microglia to the site of tissue damage. The

results presented here could have implications for both the surveillance and clearance functions of microglia following systemic infections, and the therapeutically-relevant actions of A_{2A} receptor antagonists.

Altered baseline dynamics might affect microglial surveillance functions

In this study, we treated mice with 2 mg/kg LPS peripherally to induce inflammation in the brain. The LPS treatment increased microglial activation as evident by the elevated IL-1 β and TNF- α synthesis (Figure-1A). Yet, the systemic inflammatory environment did not lead to overt cell death in the brain 48 hours post injection (Figure-1B), consistent with the idea that this LPS dose (2 mg/kg) has less profound effects than those used to model the effects of septic shock (5–10 mg/kg). It should be noted, however, that LPS treatment could induce some features of sepsis as well as have more subtle effects on neuronal physiology not detected here, such as alterations and dendritic and synaptic integrity.

Despite their apparent activation (Figure-1), microglia under LPS-induced pro-inflammatory conditions retain their ability to sample the brain parenchyma by constantly extending and retracting their processes (Suppl. Video 1). This is in accordance with microglial process extensions and retractions observed in the spinal cord of a mouse model of MS and in the cortex of an AD model (Bolmont et al. 2008; Davalos et al. 2012), confirming that microglial activation *per se* does not inhibit baseline motility. Surprisingly, the instantaneous speed of these movements is higher for microglia in LPS-treated animals than in control animals (Figure-2). Increased speed of movement for microglial processes has been previously observed in LPS-treated microglia *in vitro* (Orr et al. 2009). In spite of this hypermotile behavior, microglia in LPS-treated mice might have altered surveillance functions. The systemic activation of microglia with LPS disrupted the homogeneous coverage of the parenchyma by microglial processes (Figure-1B), and there are areas that are devoid of processes for the duration of imaging. The baseline recordings suggest that microglia do not explore these areas in the time frames examined. Hence, it is possible that microglia under inflammatory conditions might be less effective in detecting brain disturbances in non-monitored areas.

Delayed approach to tissue damage following systemic activation could affect the resolution of injuries by microglia

We examined how activated microglia respond to laser ablation *in vivo*, a previously described model of tissue damage (Davalos et al. 2005; Haynes et al. 2006). We developed MGPTracker, an algorithm to automate the quantification of microglial responses to the site of laser ablation and in this way capture the complex geometry around the ablation (Figure-4; Suppl. Video 3). Using MGPTracker, we showed that activated microglia from LPS-treated animals initially retract their processes away from the ablation site, but later respond by moving toward and surrounding the ablation (Figure-3,4; Suppl. Video 2). This result is critical in demonstrating that previous *in vitro* observations occur *in vivo*, namely that adenosine (generated from ATP breakdown) causes process retraction in activated microglia. In addition to tissue damage, elevated adenosine concentrations can be detected in several pathological conditions (Pedata et al. 2001), rendering this mechanism relevant for a broad range of neurological diseases. Some of this differential response might be due

to the altered microglial morphology following LPS activation (Figure-1B); microglial processes in LPS-treated mice appear shorter and might need to travel longer distances to reach the ablation. Thus, peripheral inflammation could alter microglial response to damage by changing both the distribution of processes and the subsequent kinetics of the response. It should be noted that the altered process distribution does not account for the initial retraction seen for LPS-activated microglia, which is a separate process induced by tissue injury.

An additional component of the delayed response could involve the P2Y₁₂ receptor. Haynes et al. (2006) reported that microglia in P2Y₁₂ knock-out animals show a delayed response to laser injury. LPS treatment downregulates P2Y₁₂ expression at both the mRNA and protein level *in vivo* (Haynes et al. 2006). Thus, the data presented here obtained in LPS-treated mice are consistent with results obtained in P2Y₁₂^{-/-} mice (Haynes et al. 2006).

It should be noted that the presence of neuroinflammation also affects microglial functions other than motility. Mice treated with intracerebral LPS can phagocytize apoptotic neurons and neutrophils (Hughes et al. 2010), which could be protective as phagocytosis is known to lower cytokine secretion by peripheral monocytes and microglia (Liu et al. 2006; Magnus et al. 2001; Voll et al. 1997). Yet, it is possible that microglia engaged in phagocytosis will be less likely to be engaged in a response to tissue damage at the same time. In this way, phagocytosis and motility may oppose each other following inflammation, further contributing to the inability of microglia to extend processes to the lesion site.

Our results show that in the presence of systemically-induced neuroinflammation, activated microglia have a delayed response to laser-induced damage *in vivo* compared to microglia in healthy brain (Davalos et al. 2005; Nimmerjahn et al. 2005) (Figure-3, 4). The initial retraction away from the tissue injury has not been described before. Yet, the laser-induced lesion model is probably more destructive in terms of the number of injured cells or processes than one might expect from slowly progressing neuronal death in neurodegenerative diseases where only a few neurons likely die at discrete time points in a given volume of tissue (Hanisch and Kettenmann 2007; McGeer et al. 1988). Moreover, the laser-induced ablation almost certainly involves the release of a large number of factors, cellular constituents, and debris that could contribute to attracting microglial processes. It therefore seems possible that the delay observed following laser ablation under inflammatory conditions might be even more pronounced as microglia respond to the cell death in the context of neurodegenerative conditions. Consistent with our findings with systemic activation, microglia in an animal model of AD, which are locally activated by the ongoing A β pathology, also show a reduced response to laser ablation (Krabbe et al. 2013). Thus, both systemic inflammation and degeneration-induced inflammation reduce the ability of microglia to respond to tissue damage *in vivo*.

Adenosine receptor antagonists affect microglial process motility *in vivo* through actions on glial A_{2A} receptors

Multiple lines of experimentation shows that A_{2A} receptor antagonists have neuroprotective properties in several neurological disorders (Melani et al. 2009; Morelli et al. 2010). The role of A_{2A} receptor antagonists has been studied most extensively in Parkinson's disease, with both epidemiological data with caffeine and work in preclinical animal models showing

a protective effect of A_{2A} receptor antagonists (Morelli et al. 2010; Schwarzschild et al. 2006; Xu et al. 2005). As a result, selective A_{2A} receptor antagonists, including preladenant, are in clinical development for the treatment of PD (Barkhoudarian and Schwarzschild 2011; Schwarzschild et al. 2006; Xu et al. 2005).

There is ongoing debate whether the neuroprotective properties of A_{2A} antagonists are mediated through neuronal or glial A_{2A} receptors, with divergent results coming from different PD models (Carta et al. 2009; Morelli et al. 2010; Xiao et al. 2006; Yu et al. 2008). Here we show for the first time that A_{2A} receptor antagonists can modulate the process dynamics of microglia *in vivo*. A₁ and A₃ receptors, which influence motility of resting microglia (Färber et al. 2008; Ohsawa et al. 2012), did not affect the dynamics of activated microglia *in vitro* (Figure-6E,F). Both caffeine and preladenant prevented adenosine-induced process retraction in activated microglia *in vitro* (Figure-6G,H). Moreover, preladenant, currently in clinical trials for Parkinson's disease (Barkhoudarian and Schwarzschild 2011; Hauser et al. 2011), partially restored microglial responses to tissue damage in the presence of inflammation *in vivo* (Figure-7,8). Thus, at least some of the neuroprotective properties of A_{2A} receptor antagonists, including caffeine and preladenant, might be explained by inhibition of microglial A_{2A} receptors. Compounds that enhance the ability of microglia to respond to brain disturbances, especially under pro-inflammatory conditions, might be good targets for the prevention or treatment of neurodegenerative diseases and other CNS conditions with chronic inflammation.

While we used LPS as a means for microglial activation in both of the *in vivo* and *in vitro* studies, the mechanism of action of LPS on microglia is different in the two preparations. *In vitro*, LPS directly activates microglia through microglial toll-like receptors. However, LPS does not cross the blood-brain barrier. Thus, an intraperitoneal injection of the endotoxin likely induces a secondary inflammatory reaction through activation of cytokine secretion by endothelial cells in the brain microvasculature (Perry et al. 2007; Perry et al. 2003). Interestingly, preladenant had similar effects on microglial motility in both preparations (Figure-6G,H,7,8), indicating that it could have meaningful effects in the context of neuroinflammation that results from different conditions.

Finally, non-steroidal anti-inflammatory drugs (NSAIDs) also have neuroprotective properties (Etminan et al. 2003; Gao et al. 2011). The effects of NSAIDs on microglial function have not been studied extensively, but they might indirectly shift microglia to a phenotype that is closer to their resting state (with reduced A_{2A} receptor expression) by inhibiting COX-2-mediated inflammation in the periphery or the brain. As a result, the neuroprotective properties of NSAIDs and A_{2A} receptor antagonists likely involve different mechanisms at different stages of disease progression. Moreover, most studies that describe a protective role of A_{2A} receptor blockade in PD and other conditions examined only the chronic effects of A_{2A} receptor antagonists, with outcome measures assessed days after antagonist administration (Carta et al. 2009; Chen et al. 2001; Xiao et al. 2006; Yu et al. 2008). However, acute effects on motor performance have also been shown (Jones et al. 2012). In the current study, we show that preladenant alters microglial motility in the minutes/hours after tissue damage. Therefore, it is possible that preladenant could have multiple mechanisms of action at multiple time points. It could initially affect the motility of

microglial processes, but later alter other microglial functions such as phagocytosis and cytokine secretion. The ability of preladenant to modify other microglial functions warrants further investigation to better understand the roles of microglia and identify novel mechanisms for modulating their functions in various disease paradigms.

Supplementary Material

Refer to Web version on PubMed Central for supplementary material.

Acknowledgments

We would like to thank Drs. H.J. Sommer III (Pennsylvania State University) and Moshe Lindner (Bar-Ilan University, Israel) for allowing us to use code developed by them for the algorithms presented here. Dr. Sommer initially developed the “polygeom.m” function to find the center of an image, and Dr. Lindner developed “image2animation.m” which makes a movie from still images. We also thank Dr. Nicholas Varvel, Jing Zhang and Lauren Shapiro (Emory University) for help with FluoroJade staining. Funding was provided by the Pharmacological Sciences Institutional Training Grant T32GM008602 to S.G., Toxicology Institutional Training Grant T32ES12870 to S.G., NINDS NRSA F31NS076215 to S.G., internal pilot grant from the Udall Parkinson’s Disease Research Center at Emory University (NIH/NINDS P50-NS071669) to S.F.T, a Young Investigator Award from the Nancy Davis Foundation for Multiple Sclerosis to D.D., and NIH/NINDS grants NS052189 and NS066361 to K.A.

References

- Akiyama H, Barger S, Barnum S, Bradt B, Bauer J, Cole GM, Cooper NR, Piet E, Emmerling M, Fiebich BL, et al. Inflammation and Alzheimer’s disease. *Neurobiology of Aging*. 2000; 21:383–421. [PubMed: 10858586]
- Barkhoudarian MT, Schwarzschild MA. Preclinical jockeying in the translational track of adenosine A_{2A} receptors. *Experimental Neurology*. 2011; 228:160–164. [PubMed: 21211537]
- Bolmont T, Haiss F, Eicke D, Radde R, Mathis CA, Klunk WE, Kohsaka S, Jucker M, Calhoun ME. Dynamics of the Microglial/Amyloid Interaction Indicate a Role in Plaque Maintenance. *Journal of Neuroscience*. 2008; 28:4283–4292. [PubMed: 18417708]
- Carta AR, Kachroo A, Schintu N, Xu K, Schwarzschild MA, Wardas J, Morelli M. Inactivation of neuronal forebrain A_{2A} receptors protects dopaminergic neurons in a mouse model of Parkinson’s disease. *Journal of Neurochemistry*. 2009; 111:1478–1489. [PubMed: 19817968]
- Chen J-F, Xu K, Petzer JP, Staal R, Xu Y-H, Beilstein M, Sonsalla PK, Castagnoli K, Castagnoli N, Schwarzschild MA. Neuroprotection by Caffeine and A_{2A} Adenosine Receptor Inactivation in a Model of Parkinson’s Disease. *The Journal of Neuroscience*. 2001; 21:RC143. [PubMed: 11319241]
- Colton CA, Wilcock DM. Assessing Activation States in Microglia. *CNS & Neurological Disorders-Drug Targets*. 2010; 9:174–191. [PubMed: 20205642]
- Cunningham C. Microglia and Neurodegeneration: The Role of Systemic Inflammation. *Glia*. 2013; 61:71–90. [PubMed: 22674585]
- Davalos D, Grutzendler J, Yang G, Kim JV, Zuo Y, Jung S, Littman DR, Dustin ML, Gan W-B. ATP mediates rapid microglial response to local brain injury *in vivo*. *Nature Neuroscience*. 2005; 8:752–758.
- Davalos D, Ryu JK, Merlini M, Baeten KM, Le Moan N, Petersen MA, Deerinck TJ, Smirnov DS, Bedard C, Hakoziaki H, et al. Fibrinogen-induced perivascular microglial clustering is required for the development of axonal damage in neuroinflammation. *Nature Communications*. 2012; 3:1227–1242.
- Edison P, Archer HA, Gerhard A, Hinz R, Pavese N, Turkheimer FE, Hammers A, Tai YF, Fox N, Kennedy A, et al. Microglia, amyloid, and cognition in Alzheimer’s disease: An [11C] (R)PK11195-PET and [11C]PIB-PET study. *Neurobiology of Disease*. 2008; 32:412–419. [PubMed: 18786637]

- Etminan M, Gill S, Samii A. Effect of non-steroidal anti-inflammatory drugs on risk of Alzheimer's disease: systematic review and meta-analysis of observational studies. *British Medical Journal*. 2003; 327:128. [PubMed: 12869452]
- Färber K, Markworth S, Pannasch U, Nolte C, Prinz V, Kronenberg G, Gertz K, Endres M, Bechmann I, Enjyoji K, et al. The Endonucleotidase *cd39*/ENTPDase1 Modulates Purinergic-Mediated Microglial Migration. *Glia*. 2008; 56:331–341. [PubMed: 18098126]
- Franchetti P, Cappellacci L, Marchetti S, Trincavelli L, Martini C, Mazzoni MR, Lucacchini A, Grifantini M. 2'-C-Methyl Analogues of Selective Adenosine Receptor Agonists: Synthesis and Binding Studies. *Journal of Medicinal Chemistry*. 1998; 41:1708–1715. [PubMed: 9572897]
- Fredholm BB, Irenius E, Kull B, Schulte G. Comparison of the potency of adenosine as an agonist at human adenosine receptors expressed in Chinese hamster ovary cells. *Biochemical Pharmacology*. 2001; 61:443–448. [PubMed: 11226378]
- Gallo-Rodriguez C, Ji X-d, Melman N, Siegman BD, Sanders LH, Orlina J, Fischer B, Pu Q, Olah ME, van Galen PJM, et al. Structure-Activity Relationships of *N*⁶- Benzyladenosine-5'-uronamides as A₃-Selective Adenosine Agonists. *Journal of Medicinal Chemistry*. 1994; 37:636–646. [PubMed: 8126704]
- Gao X, Chen H, Schwarzschild MA, Ascherio A. Use of ibuprofen and risk of Parkinson disease. *Neurology*. 2011; 76:863–869. [PubMed: 21368281]
- Gerhard A, Pavese N, Hotton G, Turkheimer F, Es M, Hammers A, Eggert K, Oertel W, Banati RB, Brooks DJ. In vivo imaging of microglial activation with [¹¹C](*R*)-PK11195 PET in idiopathic Parkinson's disease. *Neurobiology of Disease*. 2006; 21:404–412. [PubMed: 16182554]
- Gyoneva S, Traynelis SF. Norepinephrine Modulates the Motility of Resting and Activated Microglia via Different Adrenergic Receptors. *Journal of Biological Chemistry*. 2013; 288:15291–15302. [PubMed: 23548902]
- Hanisch U-K, Kettenmann H. Microglia: active sensor and versatile effector cells in the normal and pathologic brain. *Nature Neuroscience*. 2007; 10:1387–1394.
- Hasko G, Pacher P, Vizi ES, Illes P. Adenosine receptor signaling in the brain immune system. *Trends in Pharmacological Sciences*. 2005; 26:511–516. [PubMed: 16125796]
- Hauser RA, Cantillon M, Poucher E, Micheli F, Mok V, Onofrij M, Huyck KS, Wolski K. Preladenant in patients with Parkinson's disease and motor fluctuations: a phase 2, double blind, randomised trial. *Lancet Neurology*. 2011; 10:221–229.
- Haynes SE, Hloppeter G, Yang G, Kurpius D, Dailey ME, Gan W-B, Julius D. The P2Y₁₂ receptor regulates microglial activation by extracellular nucleotides. *Nature Neuroscience*. 2006; 9:1512–1519.
- Hodgson RA, Bertorelli R, Varty GB, Lachowicz JE, Forlani A, Fredduzzi S, Cohen-Williams ME, Higgins GA, Impagnatiello F, Nicolussi E, et al. Characterization of the Potent and Highly Selective A_{2A} Receptor Antagonists Preladenant and SCH 412348 [7-[2-[4-2,4-Difluorophenyl]-1-piperazinyl]-2-(2-furanyl)-7*H*-pyrazolo[4,3-*e*][1,2,4]triazolo[1,5-*c*]pyrimidin-5-amine] in Rodent Models of Movement Disorders and Depression. *Journal of Pharmacology and Experimental Therapeutics*. 2009; 330:294–303. [PubMed: 19332567]
- Honda S, Sasaki Y, Ohsawa K, Imai Y, Nakamura Y, Inoue K, Kohsaka S. Extracellular ATP or ADP Induce Chemotaxis of Cultured Microglia through G_{i/o}-Coupled P2Y Receptors. *Journal of Neuroscience*. 2001; 21:1975–1982. [PubMed: 11245682]
- Hughes MM, Field RH, Perry VH, Murray CL, Cunningham C. Microglia in the Degenerating Brain are Capable of Phagocytosis of Beads and Apoptotic Cells, But Do Not Efficiently Remove PrP^{Sc}, Even Upon LPS Stimulation. *Glia*. 2010; 58:2017–2030. [PubMed: 20878768]
- Hutchinson AJ, Webb RL, Oei HH, Ghai GR, Zimmerman MB, Williams M. CGS 21680C, an A₂ Selective Adenosine Receptor Agonist with Preferential Hypotensive Activity. *Journal of Pharmacology and Experimental Therapeutics*. 1989; 251:47–55. [PubMed: 2795469]
- Jiang J, Quan Y, Ganesh T, Pouliot WA, Dudek FE, Dingledine R. Inhibition of the prostaglandin receptor EP2 following status epilepticus reduces delayed mortality and brain inflammation. *Proc Nat Acad Sci USA*. 2013; 110:3591–3596. [PubMed: 23401547]
- Jones CK, Bubser M, Thompson AD, Dickerson JW, Turle-Lorenzo N, Amalric M, Blobaum AL, Bridges TM, Morrison RD, Jadhav S, et al. The Metabotropic Glutamate Receptor 4-Positive

- Allosteric Modulator VU0364770 Produces Efficacy Alone and in Combination with L-DOPA or and Adenosine 2A Antagonist in Preclinical Rodent Models of Parkinson's Disease. *Journal of Pharmacology and Experimental Therapeutics*. 2012; 340:404–421. [PubMed: 22088953]
- Jung S, Aliberti J, Graemmel P, Sunshine MJ, Kreutzberg GW, Sher A, Littman DR. Analysis of Fractalkine Receptor CX₃CR1 Function by Targeted Deletion and Green Fluorescent Protein Reporter Gene Insertion. *Molecular and Cellular Biology*. 2000; 20:4106–4114. [PubMed: 10805752]
- Kettenmann H, Kirchhoff F, Verkhratsky A. Microglia: New Roles for the Synaptic Stripper. *Neuron*. 2013; 77:10–18. [PubMed: 23312512]
- Krabbe G, Halle A, Matyash V, Rinnenthal JL, Eom GD, Bergardt U, Miller KR, Prokop S, Kettenman H, Heppner FL. Functional Impairment of Microglia Coincides with Beta-Amyloid Deposition in Mice with Alzheimer-Like Pathology. *PLoS One*. 2013; 8:e60921. [PubMed: 23577177]
- Liu Y, Hao W, Letiembre M, Walter S, Kulanga M, Neumann H, Fassbender K. Suppression of Microglial Inflammatory Activity by Myelin Phagocytosis: Role of p47-PHOX-Mediated Generation of Reactive Oxygen Species. *Journal of Neuroscience*. 2006; 26:12904–12913. [PubMed: 17167081]
- Magnus T, Chan A, Grauer O, Toyka KV, Gold R. Microglial Phagocytosis of Apoptotic Inflammatory T Cells Leads to Down-Regulation of Microglial Immune Activation. *Journal of Immunology*. 2001; 167:5004–5010.
- McDonald, J. *Handbook of Biological Statistics*. 2. Baltimore, MD: Sparky House Publishing; 2009.
- McGeer PL, Itagaki S, Akiyama H, McGeer EG. Rate of Cell Death in Parkinsonism Indicates Active Neuropathological Process. *Annals of Neurology*. 1988; 24:574–576. [PubMed: 3239957]
- Melani A, Cipriani S, Vannucchi MG, Nosi D, Donati C, Bruni P, Giovannini MG, Pedata F. Selective adenosine A_{2A} receptor antagonism reduces JNK activation in oligodendrocytes after cerebral ischaemia. *Brain*. 2009; 132:1480–1495. [PubMed: 19359287]
- Morelli M, Carta AR, Kachroo A, Schwarzschild MA. Pathophysiological roles for purines: adenosine, caffeine and urate. *Progress in Brain Research*. 2010; 183:183–208. [PubMed: 20696321]
- Murta V, Ferrari CC. Influence of Peripheral inflammation on the progression of multiple sclerosis: Evidence from the clinic and experimental animal models. *Molecular and Cellular Neuroscience*. 2013; 53:6–13. [PubMed: 22771835]
- Neustadt BR, Hao J, Lindo N, Greenlee WJ, Stamford AW, Tulshian D, Ongini E, Hunter J, Monopoli A, Bertorelli R, et al. Potent, selective, and orally active adenosine A_{2A} receptor antagonists: Arylpiperazine derivatives of pyrazolo[4,3-*e*]-1,2,4- triazolo[1,5-*c*]pyrimidines. *Bioorganic & Medicinal Chemistry Letters*. 2007; 17:1376–1380. [PubMed: 17236762]
- Nimmerjahn A, Kirchhoff F, Helmchen F. Resting Microglial Cells Are Highly Dynamic Surveillants of Brain Parenchyma in Vivo. *Science*. 2005; 308:1314–1318. [PubMed: 15831717]
- Ohsawa K, Sanagi T, Nakamura Y, Suzuki E, Inoue K, Kohsaka S. Adenosine A₃ receptor is involved in ADP-induced microglial process extension and migration. *Journal of Neurochemistry*. 2012; 121:217–227. [PubMed: 22335470]
- Orr AG, Orr AL, Li X-J, Gross RE, Traynelis SF. Adenosine A_{2A} receptor mediates microglial process retraction. *Nature Neuroscience*. 2009; 12:872–878.
- Pedata F, Corsi C, Melani A, Bordoni F, Latini S. Adenosine Extracellular Brain Concentrations and Role of A_{2A} Receptor in Ischemia. *Annals New York Academy of Sciences*. 2001; 939:74–84.
- Perry VH, Cunningham C, Holmes C. Systemic infections and inflammation affect chronic neurodegeneration. *Nature Reviews Immunology*. 2007; 7:161–167.
- Perry VH, Newman TA, Cunningham C. The impact of systemic infection on the progression of neurodegenerative disease. *Nature Reviews Neuroscience*. 2003; 4:103–112.
- Prinz M, Priller J, Sisodia SS, Ransohoff RM. Heterogeneity of CNS myeloid cells and their roles in neurodegeneration. *Nature Neuroscience*. 2011; 14:1–9.
- Qin L, Wu X, Block CML, Liu Y, Breese GR, Hong J-S, Knapp DJ, Crews FT. Systemic LPS Causes Chronic Neuroinflammation and Progressive Neurodegeneration. *Glia*. 2007; 55:453–462. [PubMed: 17203472]

- Schwarzschild MA, Agnati L, Fuxe K, Chen J-F, Morelli M. Targeting adenosine A_{2A} receptors in Parkinson's disease. *Trends in Neurosciences*. 2006; 29:647–654. [PubMed: 17030429]
- Semmler A, Frisch C, Debier T, Ramanathan M, Okulla T, Klockgether T, Heneka MT. Long-term cognitive impairment, neuronal loss and reduced cortical cholinergic innervation after recovery from sepsis in a rodent model. *Experimental Neurology*. 2007; 204:733–740. [PubMed: 17306796]
- Semmler A, Hermann S, Mormann F, Weberpals M, Paxian SA, Okulla T, Schäfers M, Kummer MP, Klockgether T, Heneka MT. Sepsis causes neuroinflammation and concomitant decrease of cerebral metabolism. *Journal of Neuroinflammation*. 2008; 5:38. [PubMed: 18793399]
- Semmler A, Okulla T, Sastre M, Dumitrescu-Ozimek L, Heneka MT. Systemic inflammation induces apoptosis with variable vulnerability of different brain regions. *Journal of Chemical Neuroanatomy*. 2005; 30:144–157. [PubMed: 16122904]
- Tansey MG, Goldberg MS. Neuroinflammation in Parkinson's disease: Its role in neuronal death and implications for therapeutic intervention *Neurobiology of Disease*. 2010; 37:510–518.
- Tremblay M-E, Stevens B, Sierra A, Wake H, Bessis A, Nimmerjahn A. The Role of Microglia in the Healthy Brain. *Journal of Neuroscience*. 2011; 31:16064–16069. [PubMed: 22072657]
- Venneti S, Lopresti BJ, Wiley CA. Molecular Imaging of Microglia/Macrophages in the Brain. *Glia*. 2013; 61:10–23. [PubMed: 22615180]
- Voll RE, Herrmann M, Roth EA, Stach C, Kalden JR. Immunosuppressive effects of apoptotic cells. *Nature*. 1997; 390:350–351. [PubMed: 9389474]
- von Kugelgen I, Wetter A. Molecular pharmacology of P2Y-receptors. *Naunyn-Schmiedeberg's Archives of Pharmacology*. 2000; 362:310–323.
- Weberpals M, Hermes M, Hermann S, Kummer MP, Terwel D, Semmler A, Berger M, Schäfers M, Heneka MT. *NOS2* Gene Deficiency Protects from Sepsis-Induced Long-Term Cognitive Deficits. *Journal of Neuroscience*. 2009; 29:14177–14184. [PubMed: 19906966]
- Xiao D, Bastia E, Xu Y-H, Benn CL, Cha J-HJ, Peterson TS, Chen J-F, Schwarzschild MA. Forebrain Adenosine A_{2A} Receptors Contribute to L-3,4-Dihydroxyphenylalanine-Induced Dyskinesia in Hemiparkinsonian Mice. *Journal of Neuroscience*. 2006; 26:13548–13555. [PubMed: 17192438]
- Xu K, Bastia E, Schwarzschild MA. Therapeutic potential of adenosine A_{2A} receptor antagonists in Parkinson's disease. *Pharmacology & Therapeutics*. 2005; 105:267–310. [PubMed: 15737407]
- Yu L, Shen H-Y, Coelho JE, Araujo IM, Huang Q-Y, Day Y-J, Rebola N, Canas PM, Rapp EK, Ferrara J, et al. Adenosine A_{2A} Receptor Antagonists Exert Motor and Neuroprotective Effects by Distinct Cellular Mechanisms. *Annals of Neurology*. 2008; 63:338–346. [PubMed: 18300283]
- Zimmermann H. Signalling via ATP in the nervous system. *TINS*. 1994; 17:420–426. [PubMed: 7530880]

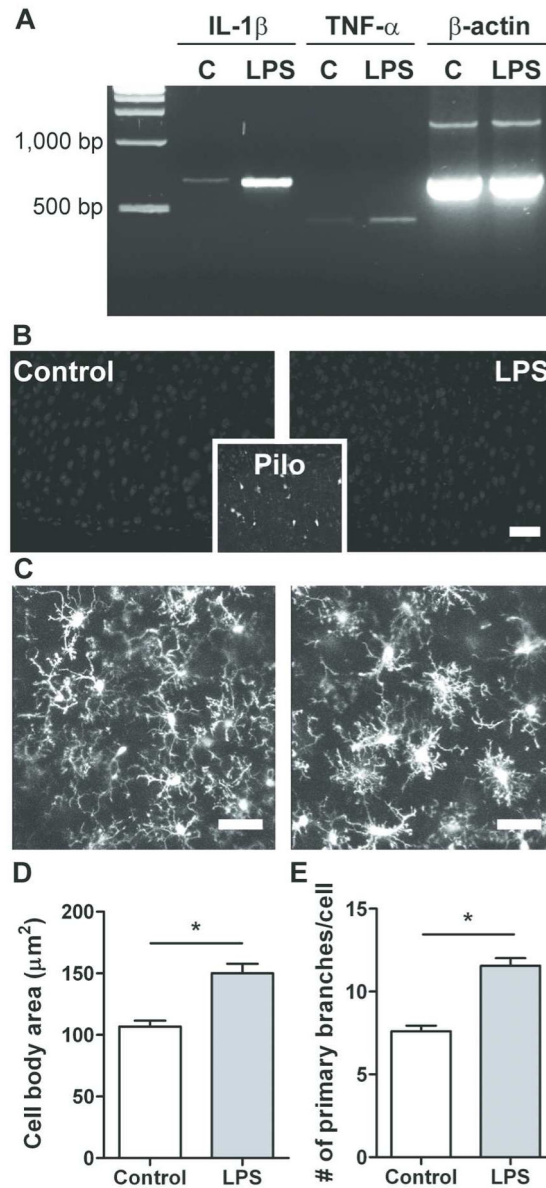


Figure 1.

Confirmation of microglial activation *in vivo*. $CX_3CR1^{GFP/+}$ mice treated with 2 mg/kg LPS i.p. were examined for the presence of neuroinflammation 2 days later. **A**. Expression of the pro-inflammatory cytokines IL-1 β and TNF- α , as determined with RT-PCR, increased following LPS treatment. Representative images from one of three PBS- (control, C) or LPS-injected animals for each treatment are shown. **B**. FluoroJade staining shows that PBS or peripheral LPS treatment (2 mg/kg) do not induce cell death in the cortex (side panels). In parallel, control experiments, pilocarpine (pilo) produced strong cell death (inset). $n=3$ mice each for LPS and PBS. Scale bar: 50 μm . **C**. 2D projections of a 30 μm section from the cortex of control ($n=9$) and LPS-injected ($n=11$) mice showing altered microglial morphology. Scale bar: 50 μm . Increase in the cell body area (**D**) and the number of primary

processes (**E**) are morphological changes consistent with microglial activation. Statistics: Student's *t*-test, *, $p < 0.05$.

Author Manuscript

Author Manuscript

Author Manuscript

Author Manuscript

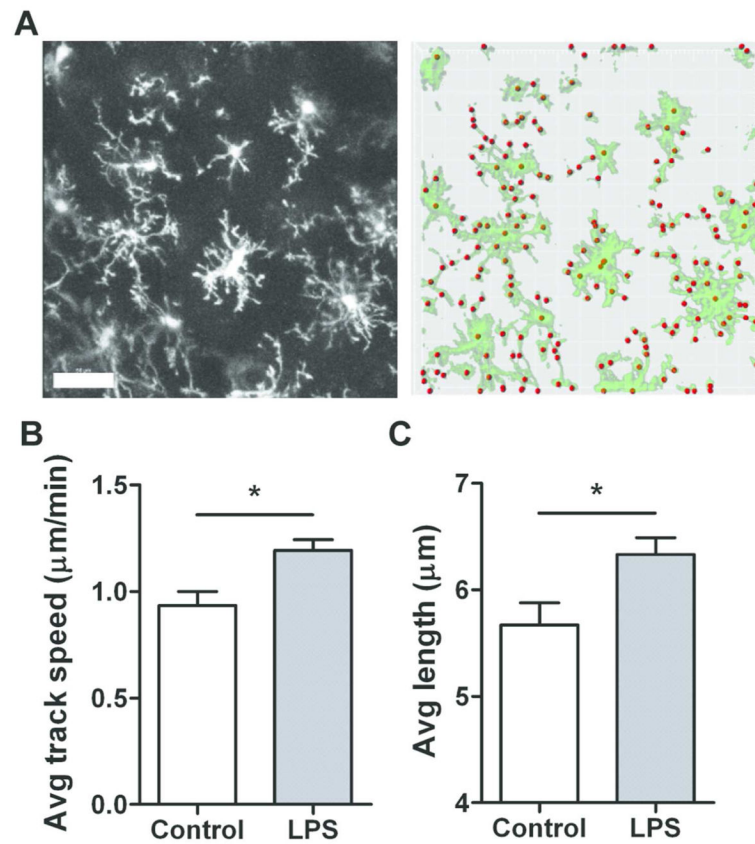


Figure 2.

Microglial motility under baseline conditions *in vivo*. **A.** The baseline motility of microglia was assessed with time-lapse 2P imaging of control (n=9) or LPS-injected (n=11) *CX₃CR1^{GFP/+}* mice. 2D projections of the cortex spanning ~30 μm vertical distance were analyzed with Imaris software to quantify baseline process dynamics. The figure shows a representative image of microglia in a LPS-injected mouse. Red dots denote objects identified by the software and tracked over time. Scale bar: 50 μm. The average track speed (**B**) and distance traveled (**C**) increased in magnitude following microglial activation. Statistics: Student's *t*-test, *, *p*<0.05.

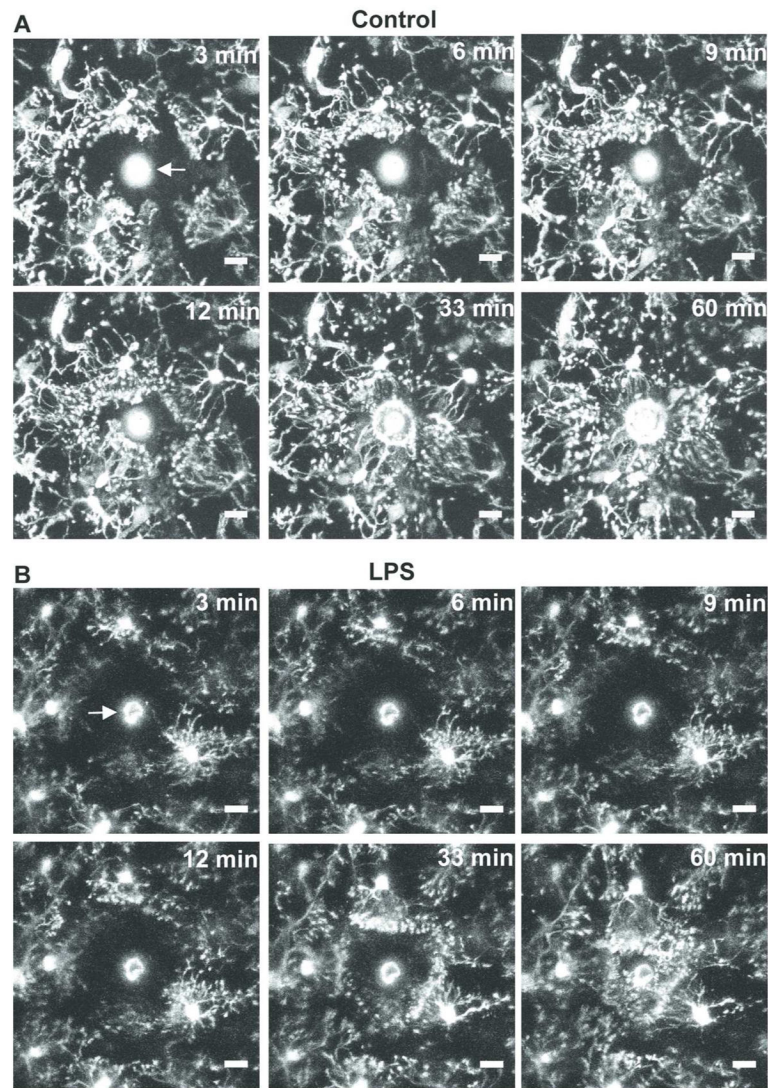


Figure 3. Microglial response to laser-induced tissue damage under resting and pro-inflammatory conditions *in vivo*. Select images from time-lapse 2P recordings from (A) control (n=9) and (B) LPS-injected (n=11) $CX_3CR1^{GFP/+}$ mice show that activated microglia in LPS-treated animals have a delayed response to laser-induced tissue damage. Arrow in first image (t=3 min) points to the location of the laser ablation. Scale bar: 20 μm .

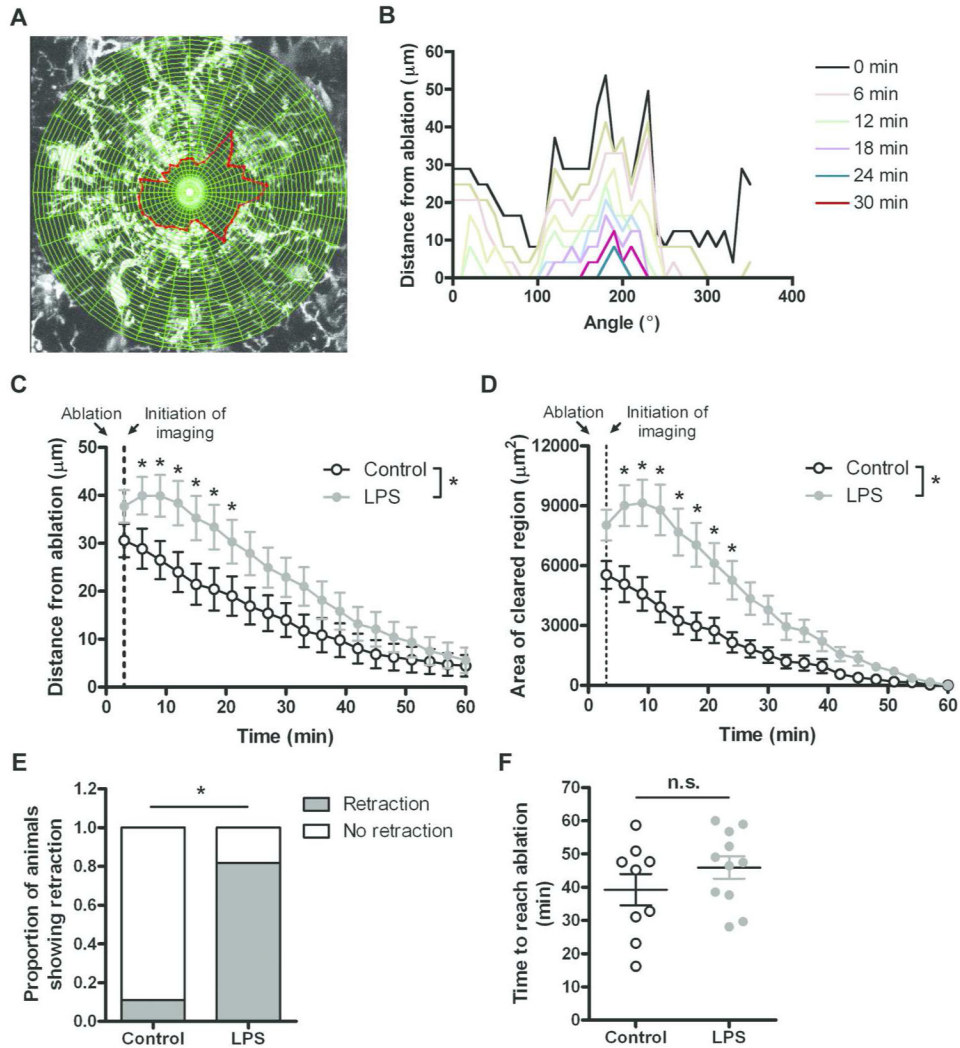


Figure 4. Quantification of microglial response to laser-induced tissue damage *in vivo*. Time-lapse 2P recordings from control (n=9) and LPS-injected (n=11) *CX₃CR1^{GFP/+}* mice were analyzed with MGPtracker, a custom-written Matlab code to quantify the approach of microglial process to the site of damage. **A.** An example of detection of microglial processes; the green radial lines divide the image in 36 sectors. The vertices of the red polygon correspond to the microglial processes closest to the ablation in each sector. **B.** Positions of the vertices of the front-tracking polygon at different time points. **C, D.** The average distance of the polygon from the ablation site (**C**), and the average area bound by the polygon (**D**) over time show different rates of approach to the ablation following microglial activation with LPS. Statistics: two-way ANOVA with Bonferroni's *post hoc* test, *, p<0.05 between control and LPS at the indicated time points. **E.** Proportion of control and LPS-treated animals that displayed initial retraction from the ablation site. Statistics: G-test of independence, *, p<0.05. **F.** Average time to reach the ablation in control and LPS-injected animals. Statistics: Student's *t*-test, n.s., not significant.

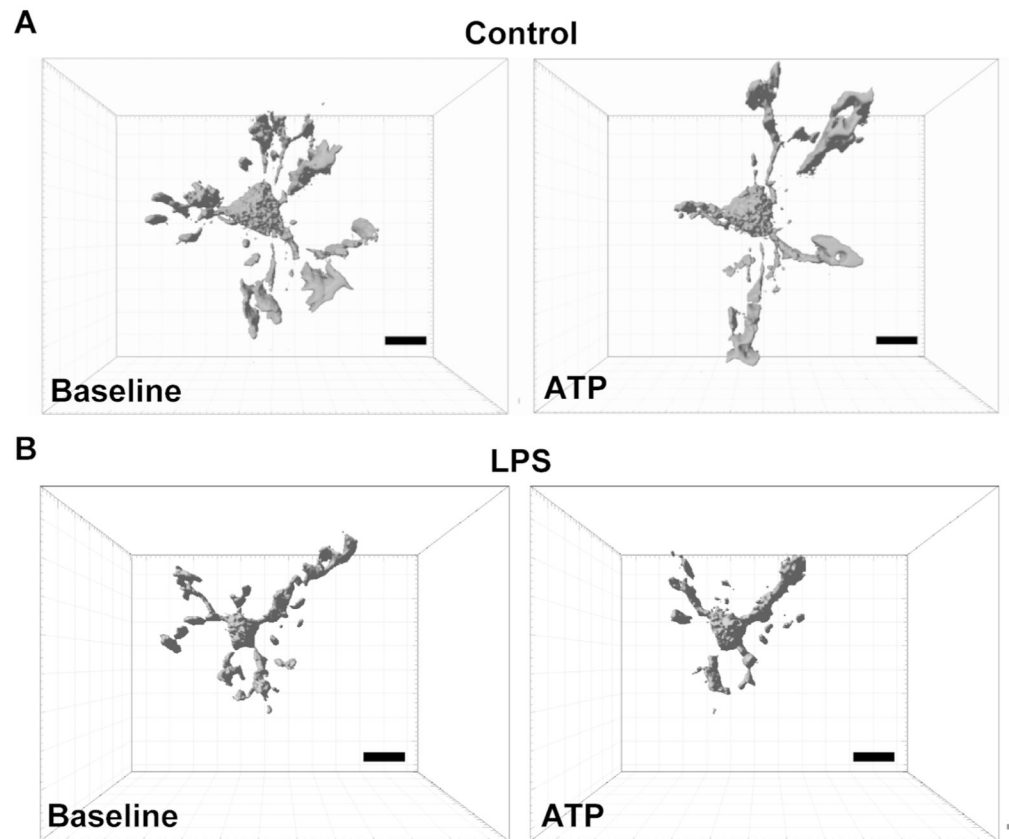


Figure 5.

Confocal imaging and 3D reconstruction of primary microglia *in vitro*. Primary microglia from *actin-GFP* mice grown in Matrigel were treated with 100 ng/mL LPS or HBSS for 24 hr. Confocal imaging over time and 3D reconstructions of the cells at each time point with the Imaris software were used to study cell ramification. The figure shows the effects of ATP treatment on cell morphology of a resting (**A**) and LPS-activated (**B**) cell: while ATP induces process extension in the resting cell, it causes retraction of processes in the LPS-activated cell. Scale bar: 10 μ m.

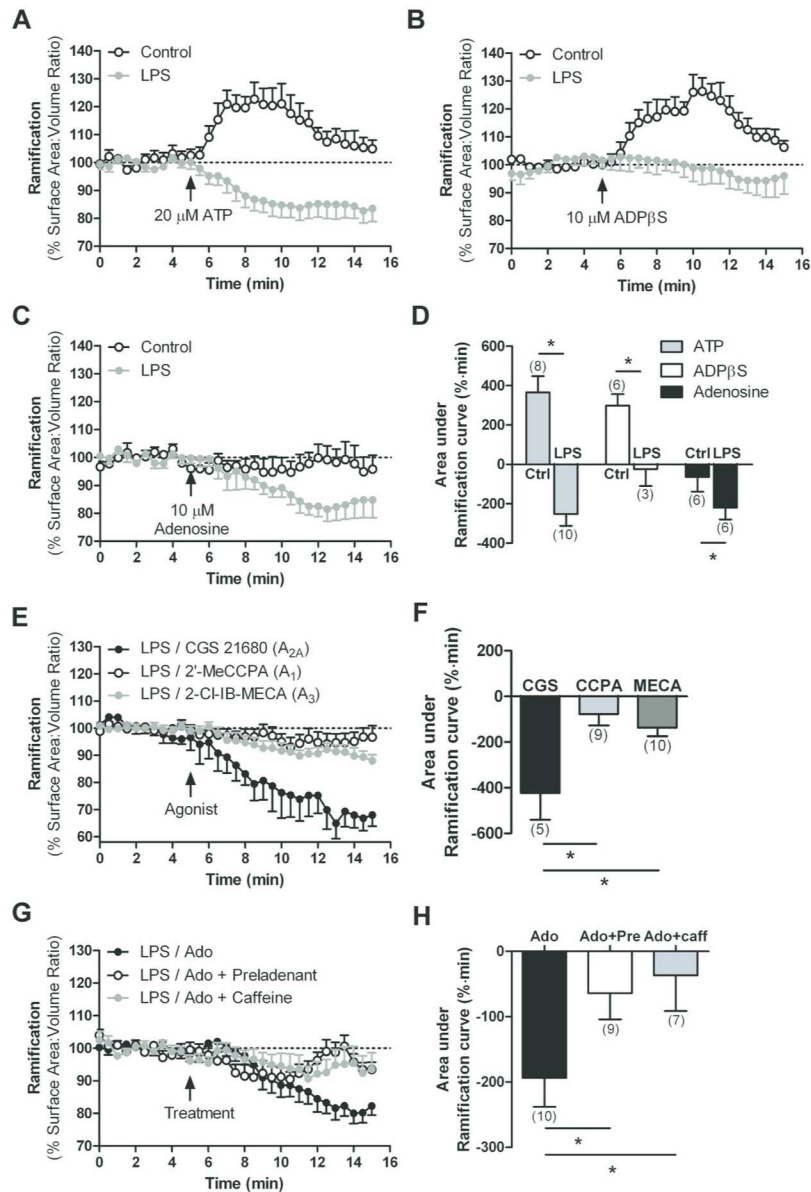


Figure 6. Mechanisms underlying microglial process retraction under pro-inflammatory conditions *in vitro*. 3D cell reconstructions from primary *actin-GFP* microglia grown in Matrigel were used to determine cell ramification (expressed as surface area-to-volume ratios) in response to different treatments. **A.** ATP application (20 μ M) exerts divergent effects on the ramification of resting and LPS-activated microglia. **B.** The non-hydrolysable P2Y₁₂ receptor agonist ADP β S (10 μ M) increases cell ramification in resting microglia only. **C.** The A_{2A} receptor agonist adenosine (10 μ M) reduces cell ramification in activated microglia only. **D.** Summary of the effects of purinergic receptor agonists on cell ramification assessed as the area under the ramification curves. Statistics: two-way ANOVA and Bonferroni's *post hoc* test (compared to control cells for each treatment), *, $p < 0.05$. **E.** The selective A₁ receptor agonist 2'-MeCCPA (1 μ M) or the selective A₃ receptor agonist 2-Cl-IB-MECA

(0.5 μM) do not affect process dynamics of activated microglia, but 3 μM of the selective A_{2A} agonist CGS-21680 induces process retraction. **F.** Summary of the effects of subtype-selective adenosine receptor agonists. Statistics: one-way ANOVA and Tukey's *post hoc* test, *, $p < 0.05$. **G.** The non-selective A_{2A} receptor antagonist caffeine (100 μM) or the selective A_{2A} receptor antagonist preladenant (1 μM) both prevent adenosine-induced process retraction in activated microglia. **H.** Summary of the effects of adenosine A_{2A} receptor antagonists. Statistics: one-way ANOVA and Tukey's *post hoc* test, *, $p < 0.05$. The number of cells for each treatment is shown in parentheses in **D**, **F**, and **H**.

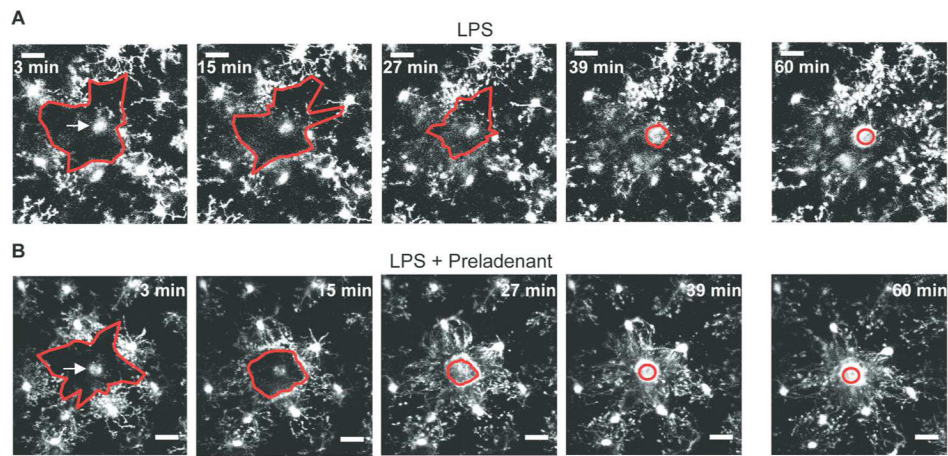


Figure 7. Microglial responses to laser-induced tissue damage following treatment with the A_{2A} receptor antagonist preladenant *in vivo*. Representative maximum intensity projections from time-lapse 2P recordings from LPS-injected $CX_3CR1^{GFP/+}$ mice before (A) and after preladenant (B) treatment (3 mg/kg, i.p., 1 hr before imaging) at different time points. Arrow in first image ($t=3$ min) points to the location of the laser ablation. Microglia appear to approach the injury site faster following preladenant injection. Scale bar: 20 μ m.

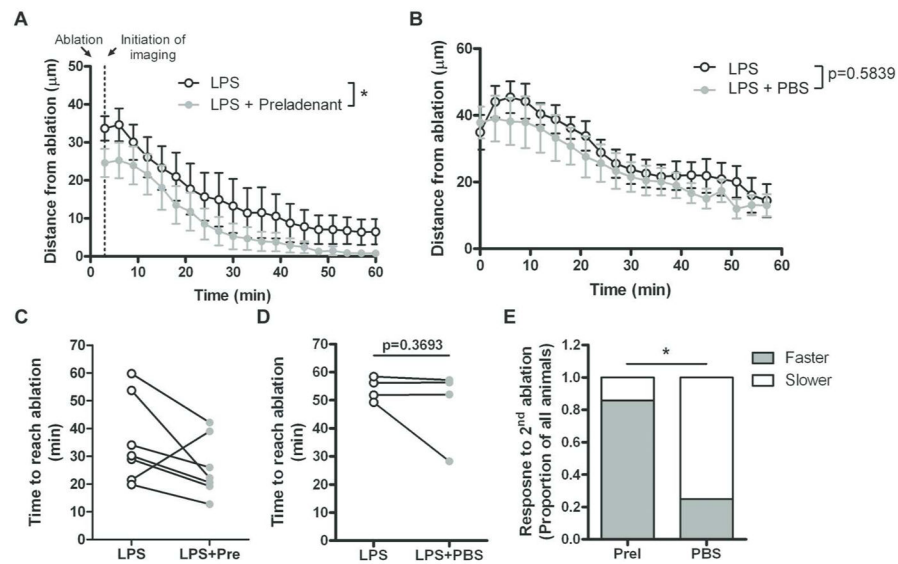


Figure 8. Quantification of microglial responses to tissue damage following preladenant treatment. **A**, **B**. Time-lapse 2P sequences from LPS-injected *CX₃CR1^{GFP/+}* mice before and after preladenant injection (n=7 mice) or control PBS injection (n=4 mice) were analyzed with MGPTracker to quantify the radial response to injury. Preladenant treatment induces a significant difference in the average distance of the polygon from the ablation site (**A**). In contrast, there is no effect of vehicle (**B**). Statistics: 2way RM-ANOVA, *, p<0.05. **C**, **D**. Time to reach the ablation before and after preladenant (**C**) or PBS (**D**) treatment. Six out of seven preladenant-treated animals show faster approach after treatment. Only one of four PBS-treated mice shows a decrease in the time to reach the ablation. Statistics: (**C**, **D**) Student's paired *t*-test. **E**. Proportion of responses that were accelerated or slowed by treatment. Statistics: G-test of independence, *, p<0.05.